Onset of Carbon Cluster Formation Inferred from Light Emission in a Laser-Induced Expansion

P. Monchicourt

Service de Physique des Atomes et des Surfaces, Centre d'Etudes Nucléaires de Saclay, 91191 Gif-sur-Yvette CEDEX, France

(Received 29 October 1990)

Space-time analysis of the light emitted from C, C_2, and C_3 has been performed in a laser-evaporated carbon expansion. The measured propagation velocities and concentration evolutions display the aggregation process as a half collision governed by momentum conservation. C_2 and C_3 clusters are produced with strong electron excitation, the energy excess of which is removed by photon emission instead of collisional cooling.

PACS numbers: 36.40.+d, 82.30.Nr

In essence, cluster formation needs the action of an efficient cooling mechanism. To this goal, supersonic jets or inert carrier gases are used extensively in order to cool the growing clusters via collisions. This scheme does not hold for carbon, which is known to produce large clusters even in high-temperature sources, such as laser-induced carbon vapors.[1] The unique and remarkable property of this element remains unexplained, especially on the question of how the clusters grow, and how the collisional energy is removed from the growing clusters. This question is approached here for C_3, which is found in various laboratory and astrophysical environments,[1] but the origin of which was not clearly established. The aim of the present work is to determine the process of cluster formation which leads to C_3. To this end, the required space-time evolutions of C, C_2, and C_3 concentrations are obtained, in a high-temperature carbon vapor, by spectroscopic means. Light emission from each of the three species allows us to follow their respective production and destruction processes, and to characterize the elementary aggregation mechanism.

Each species constituent of the carbon vapor is characterized by averages such as concentration, mean velocity, mean energy, etc., which depend on space and time and obey conservation laws. For concentrations, the rate equation is written as

$$\partial n_i(x,t)/\partial t + \nabla \cdot n_i(x,t) v_i(x,t) = S_i(x,t) - L_i(x,t) , \quad (1)$$

where $i=1$, 2, and 3 for C, C_2, and C_3, and where $n_i(x,t)$ and $v_i(x,t)$ are the local concentrations and velocities. $S_i(x,t)$ and $L_i(x,t)$ are the source and loss terms for species i. These terms are expected to couple together the different species. Next, the mean velocity $v_i(x,t)$ must fulfull the second conservation law (i.e., for momentum).[2] According to Eq. (1), the main processes governing the kinetics of species i can be determined if the number of interacting species is not too large and if $n_i(x,t)$ and $v_i(x,t)$ are simultaneously measured. This is essentially the approach used for C, C_2, and C_3 in the present work. The carbon vapor under investigation is a laser-induced expansion from graphite without carrier gas, that is, a pure carbon vapor with a limited number of interacting species. Under these conditions, the coupling between C, C_2, and C_3 is expected to appear as clearly as possible. The respective concentrations and velocities required as a function of time and space are obtained by a space-time analysis of the light emitted from the three species. This light emission will be proved in the following to be an efficient and nonperturbative diagnostic for small neutral clusters.

The measurements have been performed with the second harmonic ($\lambda=532$ nm) of a pulsed (10 Hz, 10 ns FWHM) laser (Quantel YG 581) focused through a $f=150$ cm lens on a rotating graphite rod located in a vacuum chamber (residual pressure $\lesssim 10^{-7}$ Torr). Thus, each laser pulse (estimated fluence $\sim 2\times 10^8$ W cm^{-2}) evaporates carbon from a fresh and reproducible surface, and not from a laser-deepening hole. The light emitted by the expanding vapor is analyzed as a function of space, time, and wavelength. Spatial resolution is achieved with a movable optical fiber collecting through a telescope the light emitted within a small volume ($\lesssim 1$ mm^3) downstream from the rod (0–1 cm). The light is dispersed by a monochromator (Jobin-Yvon THR 1000) over wavelengths ranging from 320 to 800 nm. The dispersed light is detected with a photomultiplier tube (Hamamatsu R928S), amplified (NF Corp 5305), and sent either to a boxcar averager (SRS 250) for spectral recording or to a digital storage oscilloscope (Le Croy 9450) for temporal analysis.

Wavelength scannings have been performed in order to identify the emitting species of the vapor. In the explored wavelength range, the spectra are dominated by C, C_2, and C_3 emission, and do not exhibit any ionic line or band. It is therefore concluded that the vapor is weakly ionized, and that small neutral species are the main constituents. The most intense atomic line is emitted at 711.6 nm and corresponds to C ($5s\,^3P, 4d\,^3F \rightarrow 3p\,^3D$) transitions. The molecular emission region —between 340 and 480 nm—is presented in Fig. 1 and shows the characteristic Swan bands ($d\,^3\Pi_g \rightarrow a\,^3\Pi_u$) of the C_2 molecule at 465–475 nm, superimposed on a large and intense continuum which peaks at 400 nm and extends from 340 to 450 nm. This spectrum reproduces

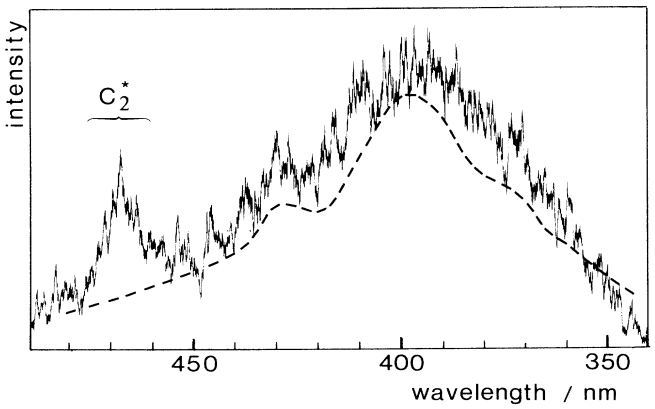

FIG. 1. A typical emission spectrum recorded with 0.8-nm resolution at 2.5 mm from the graphite rod and 500 ns after the laser pulse. This spectrum displays the Swan-band sequence $\Delta v = 1$ of the C_2 molecule at 465–475 nm, and a large and intense continuum peaking at 400 nm. This continuum is attributed to the C_3 molecule (see text). Also shown for comparison (dashed line) is the C_3 emission spectrum from an oxyacetylene flame (Ref. 4).

qualitatively the emission observed from carbon expansions cooled by a helium flow.[3] Here, however, the emission is much shorter (2 μs in time and 1 cm in spatial extension). Also, red and infrared blackbody emission from large carbon particles is completely absent. These two differences show that under the present free-expansion conditions the lifetime of the carbon plume is too brief to allow large-cluster formation. The intensity of the observed continuum depends on position, time delay, and laser intensity, but its shape remains unaltered, with the same space-time variation over the range 340–450 nm. Therefore, this wide and intense emission is due to a single species. As the central wavelength matches the $\Sigma_g^+(0,0,0) \rightarrow \Pi_u(0,0,0)$ vibronic transition of C_3,[1] and as the spectral shape fits remarkably well with C_3 emission from oxyacetylene flames, we have assigned this continuum to the C_3 molecule. This attribution agrees with the previous C_3 spectrum,[4] also shown in Fig. 1 for comparison. The absence of clear band structure for those two spectra, which contrasts with C_3 comet emission,[5] has already been observed in flames, furnaces, and other high-temperature sources.[6] In these sources, as in the present one, the excitation of a large number of closely spaced rovibronic levels which overlap results in this pseudocontinuum emission. Moreover, the velocity of the emitting particles will be seen in the following to correspond to the mass of the C_3 molecule.

The space-time evolutions of C^*, C_2^*, and C_3^* have been monitored at 711.6, 468, and 405 nm, respectively. The emission is not modified when charged particles are extracted from the vapor by a strong field (350 V cm^{-1}) applied over the whole expansion, and orthogonal to it. Therefore, the emitting levels are not populated from ionic species via recombination, but rather by inelastic

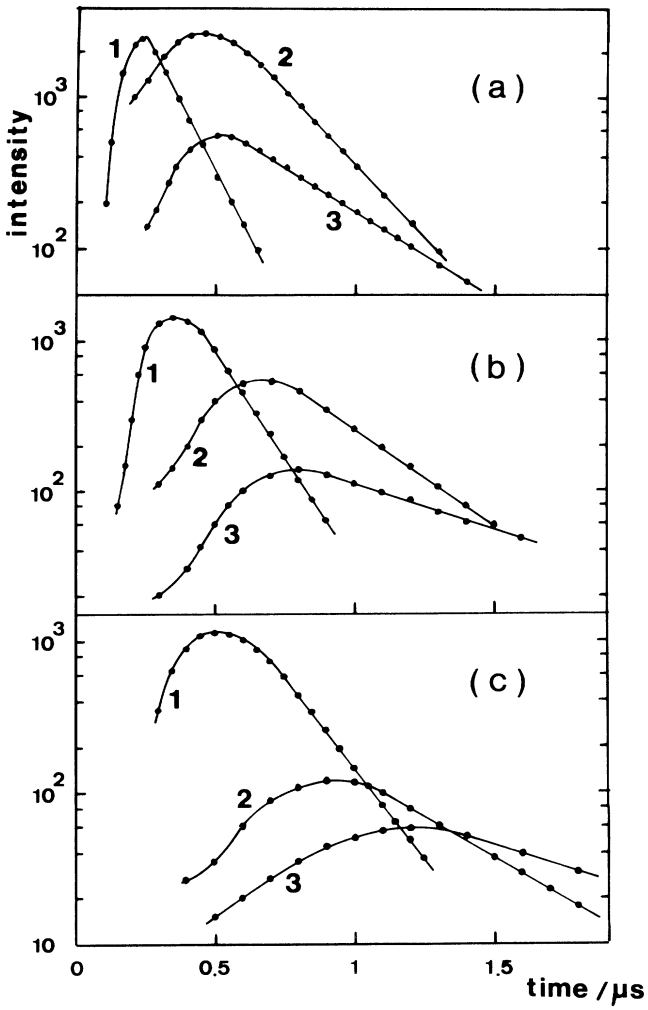

FIG. 2. Temporal emission profiles for C^*, C_2^*, and C_3^*, denoted 1, 2, and 3, at three positions along the expansion: (a) $x \simeq 0$ mm, (b) $x = 2.5$ mm, and (c) $x = 5$ mm. The logarithmic scale used for intensity shows the exponential decay for the three species. Each curve is averaged over 1000 laser shots.

collisions from neutral species. Temporal evolutions of C^*, C_2^*, and C_3^* have been obtained for various distances x and are reported for $x = 0$, 2, and 5 mm in Figs. 2(a), 2(b), and 2(c): After a first increase, an exponential decrease is observed in the three populations, together with quite different growth, position of the maximum, and decay for each species. Three important features can be deduced from these evolutions.

(i) The position of maximum intensity propagates linearly with time: This rules out a diffusive, i.e., collision-dominated, propagation ($x \propto \sqrt{t}$ in that case). The propagation velocities ($\propto x/t$) are constant over the expansion and are, respectively, $v_1 = 2 \times 10^6$, $v_2 = 10^6$, and $v_3 = 6.5 \times 10^5$ cm s^{-1} for C^*, C_2^*, and C_3^*, i.e., distributed as their mass inverse. The same ratio $1 : \frac{1}{2} : \frac{1}{3}$ for $v_1 : v_2 : v_3$ is invariably obtained, with a remarkable repro-

ducability ($<10\%$) for different laser-irradiation conditions. As the position of maximum emission coincides, for each species, with the maximum of the spatial profile ($\partial n_i/\partial t = \nabla n_i = 0$ observed at the same time), the measured velocities are the propagation velocities of the emitting particles. Therefore, Eq. (1) becomes

$$\partial n_i/\partial t + v_i \cdot \nabla n_i = S_i - L_i , \quad (1')$$

where each v_i is constant over the expansion, and such that $m_1 v_1 = m_2 v_2 = m_3 v_3$. This result leads to the statement that the velocities are governed by momentum conservation, and not by energy balance (the latter giving $m_i^{1/2} v_i = \text{const}$).

(ii) The decay time constants τ_i scale, for $x \simeq 0$, as v_i^{-1}. This implies a convective decay regime with $S_i - L_i \sim 0$ in Eq. (1'). In this regime, the temporal decay of species i, at a fixed position, is controlled by the propagation of the density profile, and not by a local loss term.

(iii) The temporal growth of C_2^* and C_3^* concentrations is seen to be triggered by the C^* population: At any position, the C_2^* and C_3^* signals begin to rise when C^* has its maximum amplitude. After this maximum, the C^* population suffers a convective decay $n_1 \sim e^{-t/\tau_1}$, whereas C_2^* grows as $n_2 \sim 1 - e^{-t/\tau_1}$. Hence, the observed growth of C_2^* is due to a local production from C atoms with velocity v_1, and not to a convective growth (at velocity v_2) from upstream population.

For C_3^*, the population grows also as $1 - e^{-t/\tau_1}$ for $x \leq 2.5$ mm, and as $1 - e^{-t/\tau_2}$ for $x > 2.5$ mm. The source of C_3^* is apparently changing from C to C_2 as the distance increases.

These three important features bring a direct answer to the question of how C_2^* and C_3^* are produced. First, they cannot be ejected from larger fragments. Second, they cannot be formed on—or ejected from—the graphite surface and gain impulsion in the expansion through a shock[7] or a Knudsen layer;[8] in that case, the directed velocity for species i with mass m_i would have had to be extracted from thermal energy and would scale as $m_i^{-1/2}$. So, they are formed along the path of carbon atoms expanding with velocity v_1 into a carbon vapor with a much slower velocity v_0. During their travel, the "fast" atoms suffer associative collisions, or "half collisions," leading to C_2^* formation,

$$C(v_1) + C(v_0) \rightarrow C_2^*(v_2) , \quad (2)$$

where momentum conservation requires $m_1 v_1 + m_1 v_0 = 2 m_1 v_2$, and yields $v_2 = \frac{1}{2}(v_1 + v_0) \approx \frac{1}{2} v_1$.

For C_3^* the most probable channel is

$$C_2(v_2) + C(v_0) \rightarrow C_3^*(v_3) \quad (3a)$$

with $v_3 = \frac{1}{3}(2v_2 + v_0) \approx \frac{1}{3} v_1$, whereas

$$C(v_1) + C(v_0) + C(v_0) \rightarrow C_3^*(v_3) \quad (3b)$$

with $v_3 = \frac{1}{3}(v_1 + 2v_0) \approx \frac{1}{3} v_1$ seems unlikely, as shown in the following discussion. This aggregation scheme is the only one able to reproduce the measured velocity ratio (with $v_0 \ll v_1$ as a necessary condition), together with the space-time evolution of the three emitting species. It involves, as seeding units for aggregation, C atoms with $v_1 \sim 2 \times 10^6$ cm s^{-1}, that is, with high kinetic energy $\frac{1}{2} m_1 v_1^2 \sim 25$ eV. Obviously, energy needs to be conserved within this scheme, and this is achieved only with strong electron excitation. The C_2^* formation from two ground-state atoms requires $\frac{1}{2} m_1 (v_1^2 + v_0^2) = \frac{1}{2} m_2 v_2^2 + \Delta E_2$, with $v_2 = \frac{1}{2}(v_1 + v_0)$. Therefore, the energy $\Delta E_2 = \frac{1}{4} m_1 v_1^2 (1 - v_0/v_1)^2 = (12.5 \text{ eV})(1 - v_0/v_1)^2$ has to be released as internal energy in the C_2 molecule. However, this energy cannot exceed the ionization threshold of C, i.e., $\Delta E_2 < 11.3$ eV. This leads, in addition to $v_0/v_1 \ll 1$, to a second condition: $v_0/v_1 > 5 \times 10^{-2}$. This condition for C_2^* formation holds for two initial ground-state atoms. Excited states of C cannot be the source of C_2^* and C_3^* because they have too much internal energy to lead to a stable neutral molecule (in this case ΔE_2 has to be increased by the initial excitation energy). Thus, the C^* emission monitored in our experiment comes from atoms which are not involved in the aggregation process, but which have to be considered as a detectable sample of a larger population evaporated from the graphite and predominantly in the ground state. Similarly, energy conservation for C_3^* formation gives $\Delta E_3 = (4 \text{ eV}) \times (1 - v_0/v_1)^2$ for process (3a), and $(17 \text{ eV})(1 - v_0/v_1)^2$ for process (3b). As the ionization threshold for C_2 is ~ 12 eV, one may conclude that process (3a) occurs for any ratio $v_0/v_1 > 0$, whereas process (3b) is very unlikely.

As the present aggregation scheme introduces the presence of "slow" carbon atoms along the path of the "fast" population, one may question how these slow atoms can be accounted for. A residual static background pressure in the vacuum chamber cannot be invoked. More credible is the time dependence and spatial inhomogeneity of the laser intensity. Fast atoms are likely ejected when and where this intensity is maximum, whereas slow atoms correspond to moderate intensities, i.e., to the beginning of the laser pulse and (or) to the peripheral region of the focal spot. The very different velocities of the two populations ($v_0/v_1 \ll 1$), which rapidly decouple along the expansion, determine the "lifetime" wherein processes (2) and (3) can occur. The mechanism producing these two atomic populations deals with laser-solid interaction and remains to be clearly identified. Another related question follows the explanation found for the observed $v_1 : v_2 : v_3$ ratio, and is the physical meaning of the measured absolute values ($v_1 = 2 \times 10^6$ cm s^{-1}). Part of the answer is found in the choice of experimental conditions: Our measurements have been performed for laser energies which maximize the C_2^* and C_3^* emission. According to process (2), this emission is maximum for kinetic energies leading at the same time to a stable C_2^* molecule, and to a max-

imum excitation in this molecule. This maximum occurs precisely when $v_1 \sim 2\times 10^6\ \mathrm{cm\,s^{-1}}$. For higher velocities, there is too much energy in the collision to produce a neutral molecule. As a consequence, besides the formation of C^*+C, ionization then occurs yielding $C_2^+ + e^-$ or C^*+C+e^-, depending on the kinetic energy. This velocity threshold, which leads to additional vanishing of C_2^*, as observed, may be considered as a crucial test corroborating the aggregation scheme discussed above.

In conclusion, direct light emission from C^*, C_2^*, and C_3^* in a laser-evaporated carbon expansion shows that these species propagate with uniform velocities which obey a mass inverse law. A simple nucleation scheme is unambiguously deduced, where C_2 and C_3 formation occurs by half collisions governed by momentum conservation. Strong electron excitation achieved in the process allows energy conservation and subsequent stabilization of the clusters via radiative cooling. Such a cluster formation looks unusual, as compared with the more familiar schemes which need relative velocities to be minimized. Actually, the present scheme allows us to comprehend that unique ability of carbon to form clusters without collisional cooling. It now becomes possible to deduce, from the observed growth rates of C_2 and C_3 induced by the C flux, the corresponding cross sections. An effort will be made in this direction in the near future, together with a detailed comparison of experimental and theoretical evolutions of the three species.

Fruitful discussions with J. Kupersztych have made possible the interpretation of the results and are gratefully acknowledged.

[1]An extensive survey of carbon cluster literature up to 1989 has been performed by W. Weltner, Jr., and R. J. Van Zee, Chem. Rev. **89**, 1713 (1989).

[2]L. Landau and E. Lifshitz, *Fluid Mechanics* (Pergamon, Oxford, 1982).

[3]M. Anselment, R. S. Smith, E. Daykin, and L. F. Dimauro, Chem. Phys. Lett. **134**, 444 (1987); E. A. Rohlfing, J. Chem. Phys. **89**, 6103 (1988).

[4]G. V. Marr, Can. J. Phys. **35**, 1275 (1957).

[5]L. Gausset, G. Herzberg, A. Lagerqvist, and B. Rosen, Astrophys. J. **142**, 45 (1965).

[6]N. H. Kiess and H. P. Broida, Can. J. Phys. **34**, 1471 (1956); L. Brewer and J. L. Engelke, J. Chem. Phys. **36**, 992 (1962).

[7]A. Vertes, P. Juhasz, P. Jani, and A. Czitrovszky, Int. J. Mass. Spectrom. Ion Processes **83**, 45 (1988).

[8]R. Kelly and R. W. Dreyfus, Surf. Sci. **198**, 263 (1988).